*URSI GASS 2020, Rome, Italy, 29 August - 5 September 2020*

# Smart Mobility Communication and Human Exposure to RF Fields: a Numerical Dosimetry Approach

Gabriella Tognola*(1), Barbara Masini(1), Silvia Gallucci(1), Marta Bonato(1,2), Serena Fiocchi(1), Emma Chiaramello(1), Laura Dossi(1), Marta Parazzini(1), and Paolo Ravazzani(1)
(1) Istituto di Elettronica e di Ingegneria dell'Informazione e delle Telecomunicazioni, Consiglio Nazionale delle Ricerche, Milano, Italy, 20133. Email: gabriella.tognola@ieiit.cnr.it
(2) DEIB, Politecnico di Milano, Italy, 20144

## Abstract

In-vehicle human exposure to RF fields generated by vehicle-to-vehicle (V2V) communication technology is assessed with numerical dosimetry. The exposure scenario was realistic and included a realistic 3D model of the car, multiple V2V antennas placed at the sides of the car and operated at the standard V2V communication frequency (5.9. GHz) and a phantom of an adult male placed at the driver position. The results evidenced that the Specific Absorption Rate (SAR) was not negligible only in the body parts closer to the antennas, i.e., the limbs and negligible in the head and torso of the phantom. Whole body SAR and 10g averaged local body SAR obtained both in single-antenna and multiple-antenna exposures were well below the ICNIRP limits of exposure for the general public in the 100 kHz-6 GHz band. The greatest SAR was obtained when all the antennas were operated simultaneously and was equal to 1% and 7% of the limits for whole body and local body exposures, respectively.

## 1 Introduction

Connected and automated vehicles will change the way we move, providing new services and applications, leading to enhanced road safety, travel efficiency and productivity. Specifically, the future deployment and coverage of next generation 5G networks could quickly increase the production of new connected vehicle services based on vehicle-to-vehicle (V2V) and more general vehicle-to-anything (V2X) communications, with an important impact also on the economy. It is, in fact, estimated that there are over 1.2 billion motor vehicles worldwide and the global market for connected cars is expected to grow by 270 percent by 2022. The latest report from Counterpoint Research's Internet of Things Tracker service indicates that major European economies are expected to hit nearly 100 percent connected car penetration by 2020. The main candidates for V2V and V2X communications are IEEE 802.11p (or its European version ITS-G5) and cellular-V2X (C-V2X), both operating at 5.9 GHz [1].

V2V communication is a topic of interest not only in the IT and telecommunication fields, for example for what concerns the management and optimization of the communication channels and communication protocols and the optimization of the antenna design, but also for the bioelectromagnetic community for what concerns the interaction with the human body of the RF fields generated by such a technology.

The scenario involved in the evaluation of V2V communication exposure has peculiar characteristics both for what concerns the environment (car + people inside the car) and frequencies (5.9 GHz) at which V2V communication is operated [2]. To the best of the authors' knowledge, none of the studies in the literature have addressed the topic of the assessment of human exposure in realistic V2V communication scenarios. A number of recent studies [3-8] evaluated the RF fields generated by realistic V2V antenna models operated at 5.9 GHz in realistic 3D models of the car but their interest was only in the evaluation of the effects of the antenna characteristics and position on the performance of the antennas and not on the evaluation of human exposure to the antenna fields. Vice versa, other studies [9-11] addressed the topic of in-vehicle human exposure to RF emitting devices used by car passengers. However, their attention was focused on RF sources other than V2V antennas, such as UMTS, WiMax, Bluetooth devices that were operated at frequencies (in the 2.1-2.5 GHz band) different than in V2V communication.

The present study aims to assess with a numerical dosimetry approach in-vehicle exposure to RF fields generated in a realistic V2V communication scenario that will make use of a realistic (for shape, dimension and materials) 3D model of a car, multiple V2V antennas that are operated at the typical V2V frequency and a realistic human model of a people (driver) inside the car.

## 2 Material and Methods

### 2.1 Exposure scenario

The exposure scenario is illustrated in Figure 1. It comprised a realistic 3D model of a car of small-medium size, four V2V antennas and a human phantom. The car was modelled as PEC (car body) and glass (six windows of 6 mm thickness; density: 2500 kg/m3; conductivity: 0.0043 S/m; relative permittivity: 4.82). The inside of the car was modelled as air because results from previous simulations revealed that common materials used in cars (e.g., foam

and plastics) have negligible effect on the distribution of in-vehicle electromagnetic fields [12]. The V2V antennas were modelled as quarter-wave monopoles and were operated at the frequency used in standard V2V communications (5.9 GHz) and at the maximum allowed power (30 W) [2]. The human phantom was an adult male ('Duke' model of the ViP v.1.0 family) and was put at the driver position inside the car. The dielectric characteristics of the tissues of the phantom were taken from the literature [13].

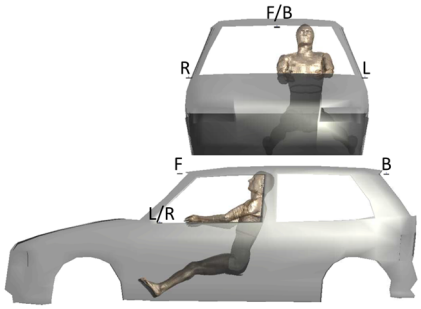


**Figure 1.** The exposure scenario. Frontal (top panel) and lateral view (bottom panel) of the realistic 3D model of the car, the human phantom and the four V2V antennas placed at the right (R), left (L), front (F), and back (B) sides of the car. Left and right antennas were placed near the car side mirrors. The dimensions of the car model are 3.8 (length) x 1.6 (width) x 1.3 m (height).

## 2.2 Simulations and exposure analysis

The electromagnetic fields and Specific Absorption Rate (SAR) induced by the V2V antennas were calculated using the finite-difference time-domain (FDTD) solver of the simulation platform SIM4life (ZMT Zurich Med Tech AG, Zurich, Switzerland, www.zurichmedtech.co). The computational domain included the car model, the four antennas and the human phantom. It was discretized with a non-uniform grid of 2 mm maximum step, which resulted in a total number of about $10^9$ cells; its boundaries were modelled as Perfectly Matching Layer (PML).

SAR was evaluated for both the average whole body exposure and for local exposure at the limbs, head and torso. Local SAR was calculated as 10g average [14] and was evaluated across the whole mass of a body region (e.g. for the entire head) and for the single tissues of a given region (e.g., the skin of the head).

As an example of the EMF generated by the V2V antennas, Figure 2 displays the electric field E due to single (left and front antenna separately) and cumulative antenna (all four antennas simultaneously) exposure. The electric field in Figure 2 was evaluated in the region surrounding the phantom, on a sagittal plane placed at the midline of the phantom. The first remark is that the electric field generated by the antennas decreased very quickly with the distance from the source. As a result, only the antennas closer to the phantom, i.e., the left and front antennas in the scenario analyzed in the present study, generated a significant electric field in the region surrounding the phantom. When all four antennas are operated simultaneously (see the bottom panel in Figure 2) the resulting distribution of the E becomes a bit more spread than that observed in single antenna exposures. The effect of exposure to all antennas is more evident in the spread of the distribution than in an increase of the magnitude of the field. The direct consequence of the exposure to all four antennas is the increase of the number of body parts with an electric field greater than in single-antenna exposure. As a matter of fact, all-antenna exposure generated a significant electric field at both the right and left forearms and (marginally) at the left leg. As a last remark, it is to note that neither single-antenna nor all-antenna exposure generated significant electric field at the head and torso of the human phantom.

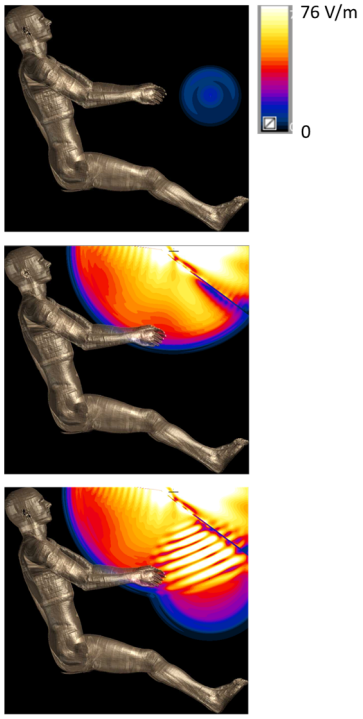


**Figure 2.** Distribution of the electric field E (rms value) generated by the left (top panel) and front antenna (mid panel) separately and by the four antennas simultaneously (bottom panel). E is evaluated on a sagittal plane at the midline of the phantom model. Color map ranges from 0 to 76 V/m (linear scale).

The highest values of SAR were obtained during the exposure to all four antennas, both in the whole body and in local body regions. Specifically, SAR averaged over the whole body was 0.78 mW/kg; the peak value of 10g average SAR in the limbs was 267 mW/kg in the left arm, 249 mW/kg in the right arm, and 32 mW/kg in the left leg. The head and torso had negligible SAR ($<<10^{-8}$ W/kg). Both whole body and local SAR were well below the ICNIRP limits of 0.08 W/kg for whole body exposure and 4 W/kg for local exposure at the limbs for the general public in the 100 kHz-6 GHz band [14].


**Figure 3.** 3D representation of the distribution of the 10g average SAR induced on the skin of the phantom by the left antenna (top panel) and front antenna (mid panel) alone and by the four antennas simultaneously (bottom panel). Color map ranges from 0 to -50 dB (re: 267 mW/kg).

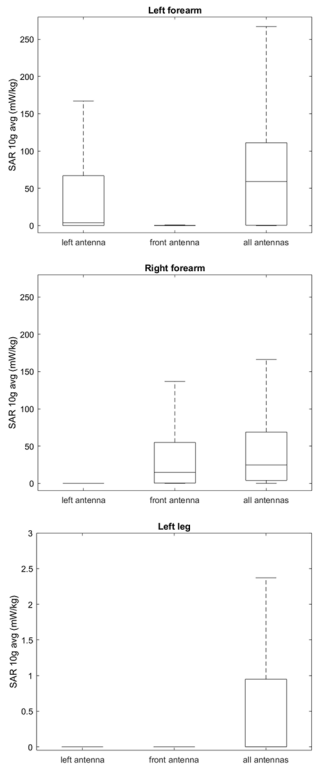


**Figure 4.** Boxplot of 10g average SAR induced in the skin of the left forearm (top panel), right forearm (bottom panel), and left leg (bottom panel) by the left and front antenna alone and by the four antennas simultaneously. Center lines in the boxes indicate the median; the bottom and top edges are the 25th and 75th percentiles. The whiskers correspond to approximately 99.3% of the values.

Significant SAR values were observed only in the most superficial tissues of the body, i.e., in the skin (and very marginally, in the subcutaneous adipose tissue). Figure 3 displays the distribution of SAR (10g average) induced on the skin of the phantom by the left and front antenna separately and by the four antennas simultaneously. Similarly to the electric field, SAR was localized only in the body regions closest to the antennas (i.e., the limbs); in these latter regions it was focused in quite narrow areas.

Lastly, Figure 4 is the boxplot representation of the 10g average SAR that was pictorially illustrated in previous Figure 3. Figure 4 shows that the exposure to all four antennas simultaneously induced a significant SAR in more body parts than the single-antenna exposure. The effect of exposure to all four antennas simultaneously was not only a slight increase of the median value of the SAR in a given body part but an even greater evident increase of the spread of SAR on the skin.

## 3 Conclusions

This paper presents the assessment of in-vehicle exposure to RF field generated by new technologies used in V2V communications. The novelty of the analysis was (i) in the use of a realistic scenario that includes a realistic model (for shape, dimension and materials) of a city car, multiple V2V antennas and an accurate phantom of a human body and (ii) in the study of the exposure in a frequency band (5.9 GHz) which has never been addressed before in a similar scenario.

The main results can be summarized as follows: (i) the electric field generated by antennas operated at 5.9 GHz rapidly decreased with the distance from the source; (ii) as a result of this behavior, the electric field was significant only in the regions closer to the antennas, i.e., at the left and right arms and the left leg; (iii) in the setup analyzed in the present study, the right and back antennas were the farthest antennas from the phantom and their electric field was negligible in the region surrounding the phantom; (iv) the head and torso were characterized by negligible values of the electric field and SAR, even when considering the simultaneous exposure to all V2V antennas mounted on the car; (v) whole body and local SAR were well below the ICNIRP limits of exposure for the general public in the 100 kHz-6 GHz band; (vi) significant values of SAR were obtained only in the skin and not in more profound tissues; (vii) the effect of simultaneous exposure to all four antennas was a (marginal) increase in the average value of SAR and an evident increase in the spread of SAR over the skin.

Many are the parameters that play an important role in the evaluation of the exposure in a V2V scenario, for example the position of the antennas and of the people inside the car together with the shape and dimension of the car. As such, it would be interesting to further explore the exposure in different V2V scenarios with non-deterministic dosimetric approaches, based e.g., on Machine Learning or stochastic

algorithms [15-16], for considering the effect of the position and number of people not only in the car but also outside the car (i.e., pedestrians), the age of the people, and the position of the antennas.

## 7 References


1. A. Bazzi, G. Cecchini, M. Menarini, B. Masini, A. Zanella, "Survey and perspectives of vehicular Wi-Fi versus Sidelink Cellular-V2X in the 5G Era," *Future Internet*, 11, p. 122, 2019.

2. IEEE Standard for Information technology-- Local and metropolitan area networks-- Specific requirements-- Part 11: Wireless LAN Medium Access Control (MAC) and Physical Layer (PHY) Specifications Amendment 6: Wireless Access in Vehicular Environments, in *IEEE Std 802.11p-2010*, pp.1-51, 2010.

3. D. Kornek, M. Schack, E. Slottke, O. Klemp, I. Rolfes and T. Kürner, "Effects of antenna characteristics and placements on a Vehicle-to-Vehicle channel scenario," in *Proc. 2010 IEEE International Conference on Communications Workshops*, Capetown, 2010, pp. 1-5.

4. M.B. Diez, P. Plitt, W. Pascher, and S. Lindenmeier, "Antenna placement and wave propagation for Car-to-Car communication," in *Proc. 2015 European Microwave Conference (EuMC)*, Paris, 2015, pp. 207-210.

5. G. Gavilanes, M. Reineri, D. Brevi, R. Scopigno, M. Gallo, M. Pannozzo, S. Bruni, and D. Zamberlan, "Comparative characterization of four antennas for VANETs by on-field measurements," in *Proc. 2013 IEEE International Conference on Microwaves, Communications, Antennas and Electronic Systems (COMCAS 2013)*, Tel Aviv, 2013, pp. 1-5.

6. E. Whalen, A. Elfrgani, C. Reddy and R. Rajan, "Antenna placement optimization for Vehicle-to-Vehicle communications," in *Proc. 2018 IEEE International Symposium on Antennas and Propagation & USNC/URSI National Radio Science Meeting*, Boston, MA, 2018, pp. 1673-1674.

7. D. Eckhoff, A. Brummer and C. Sommer, "On the impact of antenna patterns on VANET simulation," in *Proc. 2016 IEEE Vehicular Networking Conference (VNC)*, Columbus, OH, 2016, pp. 1-4.

8. G. Artner, W. Kotterman, G. Del Galdo and M.A. Hein, "Automotive Antenna Roof for Cooperative Connected Driving," *IEEE Access*, **7**, pp. 20083-20090, 2019.

9. E. Aguirre, PL. Iturri, L. Azpilicueta, S. De Miguel-Bilbao, V. Ramos, U. Gárate, and F. Falcone, "Analysis of estimation of electromagnetic dosimetric values from non-ionizing radiofrequency fields in conventional road vehicle environments," *Electromagn Biol Med*, **34**, pp. 19–28, 2015.

10. S-W. Leung, Y. Diao, K-H. Chan, Y-M. Siu, and Y. Wu, "Specific Absorption Rate evaluation for passengers using wireless communication devices inside vehicles with different handedness, passenger counts, and seating locations," *IEEE T Bio Med Eng*, **59**, pp. 2905-2912, 2012.

11. L.-R. Harris, M. Zhadobov, N. Chahat, and R. Sauleau, "Electromagnetic dosimetry for adult and child models within a car: multi-exposure scenarios," *Int J Microw Wirel T*, **3**, pp. 707–715, 2011.

12. A. Ruddle, "Influence of dielectric materials on in-vehicle electromagnetic fields," in *Proc. IET Seminar on EM Propagation in Buildings and Large Structures*, London, 2008.

13. S. Gabriel, RW. Lau, and C. Gabriel, "The dielectric properties of biological tissues: II. Measurements in the frequency range 10 Hz to 20 GHz", *Phys Med Biol*, **41**, pp. 2251-2269, 1996.

14. International Commission on Non-Ionizing Radiation Protection, "ICNIRP guidelines for limiting exposure to time-varying electric, magnetic and electromagnetic fields (up to 300 GHz)", *Health Phys*, **74**, pp. 494–522, 1998.

15. M. Bonato, E. Chiaramello, S. Fiocchi, G. Tognola, P. Ravazzani and M. Parazzini, "Influence of low frequency near-field sources position on the assessment of children exposure variability using Stochastic Dosimetry," *IEEE J Electromag RF and Microw Med Biol*, 2019 (Early Access).

16. G. Tognola, M. Bonato, E. Chiaramello, S. Fiocchi, I. Magne, M. Souques, M. Parazzini, and P. Ravazzani, Use of Machine Learning in the analysis of indoor ELF MF exposure in children", *Int J Environ Res Public Health*, **16**, p. 1230-1243, 2019.